Detecting Simulated Patterns of Lung Cancer Biomarkers by Random Network of Single-Walled Carbon Nanotubes Coated with Nonpolymeric Organic Materials

ARTICLE *in* NANO LETTERS · NOVEMBER 2008

Impact Factor: 13.59 · DOI: 10.1021/nl801577u · Source: PubMed

3 AUTHORS, INCLUDING:

Hossam Haick
Technion - Israel Institute of Technology
156 PUBLICATIONS **4,371** CITATIONS

NANO LETTERS

2008
Vol. 8, No. 11
3631-3635

Detecting Simulated Patterns of Lung Cancer Biomarkers by Random Network of Single-Walled Carbon Nanotubes Coated with Nonpolymeric Organic Materials

Gang Peng, Elena Trock, and Hossam Haick*

The Department of Chemical Engineering and Russell Barrie Nanotechnology Institute, Technion - Israel Institute of Technology, Haifa 32000, Israel

Received June 3, 2008; Revised Manuscript Received August 3, 2008

ABSTRACT

An array of chemiresistive random network of single-walled carbon nanotubes coated with nonpolymeric organic materials shows a high potential for diagnosis of lung cancer via breath samples. The sensors array shows excellent discrimination between the volatile organic compounds (VOCs) found in the breath of patients with lung cancer, relative to healthy controls, especially if the sensors array is preceded with either water extractor and/or preconcentrator of VOCs. The pattern compositions of the healthy and cancerous states were determined by gas-chromatography linked with mass-spectroscopy (GC-MS) analysis of real exhaled breath.

Recent statistics have estimated that there were nearly 3 million new cases of cancer diagnosed in 2004 and over 1.7 million deaths from cancer in Europe and the U.S. with lung cancer listed as one of the most common forms of cancer diagnosed and a leading cause of death.[1,2] Unfortunately, the most common methods currently used to diagnose lung cancer can occasionally miss tumors because they depend on tumor size. In addition, they are costly and not amenable to widespread screening because they are not efficient in terms of time.[3] In contrast, breath testing has long been recognized as a medical technique that allows diagnosis of disease by linking specific volatile organic compounds (VOCs) metabolites in exhaled breath to medical conditions. In certain instances, breath analysis offers several potential advantages: (I) breath samples are noninvasive and easy to obtain; (II) breath contains less complicated mixtures than either serum or urine; and (III) breath testing has the potential for direct and real-time monitoring.

Recent studies of gas-chromatography/mass-spectroscopy (GC-MS), mostly characterized by a detection limit of few parts per millions (ppm), linked with a ($\times 10^3-10^4$) preconcentrator have shown that several breath VOCs appear to be elevated in instances of lung cancer.[4−6] The compounds of interest are generally to be found at 1−20 parts per billion (ppb) in healthy human breath but can be seen in distinctive mixture compositions and at elevated levels from 10−100 ppb (picomolar−nanomolar concentrations) in the breath of diseased patients.[5] A discrimination between patients with and without lung cancer, regardless of the disease stage, was achieved via a combination of 22 VOCs:[6] styrene (ethenyl-benzene), 2.2.4.6.6-pentamethyl heptanes, 2-methyl heptanes, decane, propyl benzene, 1-hexene, hepatanal, 1,4-dimethyl benzene, undecane, methyl cyclopentane, 1-methyl-2-pentyl-cyclopropane, trichlorofluoro benzene, benzene, 1-methyl-ethenyl benzene, cyclohexane, 1-heptene, 1,2,4-trimethyl benzene, 2-methyl-(isoprene)-1,3-butadiene, 3-methyl octane, 1-hexene, 3-methyl nonane, hexanal, and 2,4-dimethyl heptanes. Additional evidence that lung cancer can be detected by analyzing patients' breath has been obtained from a GC column that was coupled with arrays of polymer-coated surface acoustic wave (SAW) sensors.[7] An artificial neural network was used instead of an alveolar gradient to separate the samples into healthy and diseased states. A group of VOCs characteristic of lung cancer was identified even using this relatively insensitive detector (mostly limited to a detection level of few ppm) with a breath preconcentrator being used prior to the GC column. In another study, an array of coated quartz crystal microbalance (QCM) sensors has been used without preconcentration to detect lung cancer in patients immediately prior to surgical tumor removal.[8] These latter experiments relied entirely upon the QCM (mostly having a detection limit of few ppm) array and did not use a preconcentrator of the breath. However, the analytes actually being detected by that system are currently unknown,

* To whom correspondence should be addressed. E-mail: hhossam@technion.ac.il.

10.1021/nl801577u CCC: $40.75
Published on Web 10/08/2008

and no information is available about whether this signature was independent of stage or was associated with the size of the cancerous tumor. Coated QCMs are comparable in sensitivity to coated SAW devices, but the lack of a preconcentrator in this study suggests that either different volatile biomarkers or even higher levels of VOCs were present in the patients of concern.

In this study, we have developed an array of sensors to detect lung cancer and to differentiate between the VOCs found in the breath of patients with lung cancer, relative to healthy controls. A technology in which a (semi-) conductive random network of single-walled carbon nanotubes (SWCNTs)[9−11] and insulating nonpolymeric organic materials provide arrays of chemically sensitive resistive vapor detectors form the basis for our approach. Using SWCNT networks circumvents the requirement of position and structural control (as is the case in devices based on individual SWCNT) because the devices display the averaged usual properties of many randomly distributed SWCNTs.[9−11] An additional feature of SWCNT networks is that they can be processed into devices of arbitrary size using conventional microfabrication technology.

The study was designed in three phases. In the first phase, alveolar breath was collected from individuals with lung cancer and from healthy subjects by the off-line method recommended by the ATS/ERS.[12] In this method, the subjects inhaled to total lung capacity through a mouthpiece that contained a cartridge on the inspiratory port, which removed more than 99.99% of VOCs from the air during inspiration, thus clearing the inhaled air of any ambient contaminants. Immediately after that, the subjects exhaled against 10−15 cm H_2O pressure to ensure closure of the vellum to exclude nasal entrainment of gas. The exhaled gas was collected through a separate exhalation port of the mouthpiece in a nonreactive Mylar gas-sampling bag (purchased from Eco Medics), which was previously cleaned with nitrogen gas. A minimum of five analyses was performed on the exhaled breath of each volunteer. Thirty nonsmoker people between the ages of 28−60, 15 healthy subjects and 15 individuals with stage-4 lung cancer, were volunteered and included in this study. All volunteers were previously clinically diagnosed using various diagnostic methods including bronchoscope biopsy, computed tomography (CT) scan, and pulmonary puncture. None of the lung cancer patients had received chemotherapy and/or other treatment before breath samples were collected.

In the second phase, the collected breath samples from individuals with lung cancer and from healthy subjects were analyzed with GC-MS combined with solid phase microextraction (SPME). The SPME technique was used for preconcentrating the VOCs in the breath samples. A manual SPME holder with an extraction fiber coated with polydimethylsiloxane (PDMS) (purchased from Sigma-Aldrich) was inserted into the Mylar bag. Between 500 and 1000 cm^3 of breath sample was concentrated via SPME method and delivered to GC-MS using a manual SPME holder. The extracted fiber in the manual SPME holder was inserted into injector of GC, which worked using the splitless model. The

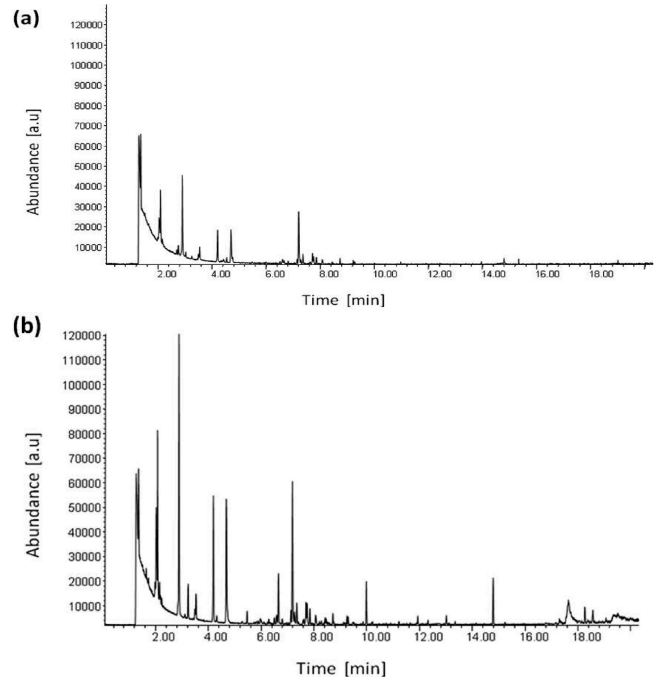

Figure 1. Representative GC-MS spectra of exhaled breath of (a) "healthy" states, and (b) patients with "lung cancer".

oven temperature profile was 60 °C, 2 min, 8 °C/min to 100 °C, 15 °C/min to 120 °C, 8 °C/min to 180 °C, 15 °C/min to 200 °C, 8 °C/min to 225 °C. Capillary column H5-5MS 5% phenyl methyl siloxane (30 m length, 0.25 mm i.d., 0.25 μm thickness) was used. The column pressure was set to 8.22 psi, and initial flow was 1.0 mL/min. Eventually, the molecular structures of the VOCs were determined via the Standard Modular Set.

The GC-MS results of breath tests identified 120−200 different VOCs that had been either synthesized or catabolized by at least one "healthy" or "cancerous" subject. Representative GC-MS spectra of exhaled breath of "healthy" states and patients with "lung cancer" are presented in Figure 1. As shown in the figure, the GC-MS analysis shows that several breath VOCs appear to be elevated in instances of lung cancer, mostly C4−C20 straight and monomethylated alkanes, in addition to certain benzene derivatives.[4−6] Forward stepwise discriminant analysis identified 15 of these VOCs as the best set of markers of disease, with >95% confidence. The compounds that were observed in both healthy (Figure 1a) and cancerous breath (Figure 1b) were presented not only at different concentrations but also in distinctive mixture compositions.[5] Representative VOCs that were presented in most lung cancer (real) samples at the highest concentration levels were simulated via homemade system (see Supporting Information, Section 3) and exposed to the developed detectors (see below). As such VOCs, trimethyl benzene, styrene, decane, octane, and 1-hexene were chosen. In addition to these representative lung cancer VOCs, water was used to simulate the saturated humidity in the exhaled breath. We use this (simulation) approach over direct exposure of the collected (real) exhaled breath to precisely determine: (I) the signature of each individual cancer volatile biomarker on the developed array of sensors;

Table 1. Sorption Materials Used in the Sensors and the Related Abbreviations[13,14]

abbreviation	sorption film
S1	propyl gallate ($c_{10}H_{12}O_5$)
S2	authracene ($c_{14}H_{10}$)
S3	tetracosanoic acid ($C_{24}H_{48}O_2$)
S4	tricosane ($c_{23}H_{48}$)
S5	3-methyl-2-phenyl valeric acid ($C_{12}H_{16}O_2$)
S6	tris(hydroxymethyl)nitro-methane ($C_4H_9NO_5$)
S7	tetracosane ($c_{24}H_{50}$)+ dioctyl phthalate(($C_{24}H_{38}O_4$) (3:1 w/w)
S8	tetracosanoic acid ($C_{24}H_{48}O_2$) + dioctyl phthalate (($C_{24}H_{38}O_4$) (3:1 w/w)
S9	1.2.5.6.9.10-hexabrormo-cyclododecane ($C_{12}H_{18}Br_6$) + dioctyl phthalate($C_{24}H_{38}O_4$) (3:1 w/w)
S10	pentadecane ($c_{15}H_{32}$) + dioctyl phthalate ($C_{24}H_{38}O_4$) (3:1 w/w)

(II) the correlation between the sensor's sensitivity and specificity of the individual VOC biomarkers to its existence in a pattern (or mixture) of other compounds; and (III) the necessary iterative feedback on sensors viability without the intervention of (disruptive) parameter, such as patients' diet, metabolic state, genetics, etc.

In the third phase of the study, an array of random network of SWCNTs were coated with variety of thin (0.5−1.0 μm in thickness) organic films and exposed to lung cancer biomarkers. Details on the fabrication and characterization of this array of sensors could be found in the Supporting Information. As (semi)chemoselective organic films for lung cancer biomarkers, we used nonpolymeric organic materials having as much as different chain length, chain branching, aromatic configuration, and functional groups (see Table 1).[13] The diversity and the increased density of the nonpolymeric functional groups ought to increase the interactions between the vapor molecules and the sorption material, as compared to polymer-based sorption phases.[14] Therefore, the nonpolymeric materials ought to produce additional increase in the sensitivity of such chemically vapor detectors in a fashion that would be very difficult to accomplish with polymer-based sorption phases.[14] Of great importance, these nonpolymeric functional materials ought to provide enhanced discrimination between closely related alkane species and will help to discriminate between closely related mixtures of alkane compounds.[14] The use of an array of such highly sorptive films therefore readily provides distinct response fingerprints for compositionally different mixtures of the VOCs, which is a requirement for differentiating between the healthy and diseased states of lung cancer.

The response ($\Delta R/R_b$, where R_b is the baseline resistance of the sensor in the absence of analyte, and ΔR is the baseline-corrected steady-state resistance change upon exposure of the sensor to analyte) of a series of SWCNT sensors to the different lung cancer biomarkers at concentrations between 10 ppb and 100 ppm was first examined. As shown in Figure 2 of the Supporting Information, the sensors' response was rapid upon exposure to vapor analyte, fully reversible upon switching back to zero vapor analyte (purified, dry air), responsive to a wide variety of concentrations, and showed a satisfying signal-to-noise ratio (typically, larger than 10:1). In general, sorption of biomarkers showed change in resistance with exposure to an analyte. While part

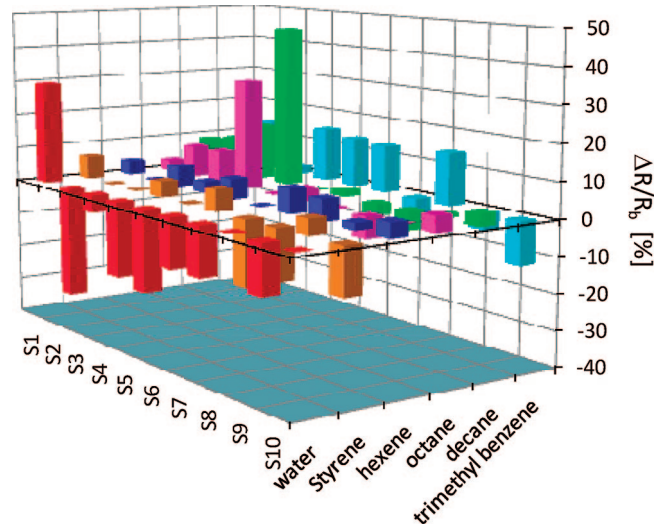

Figure 2. Response patterns for the representative VOC biomarkers. For a given sensor that is exposed to a specific analyte, the presented value of $\Delta R/R_b$ is the average of all responses obtained during the first 10 min exposure to that analyte.

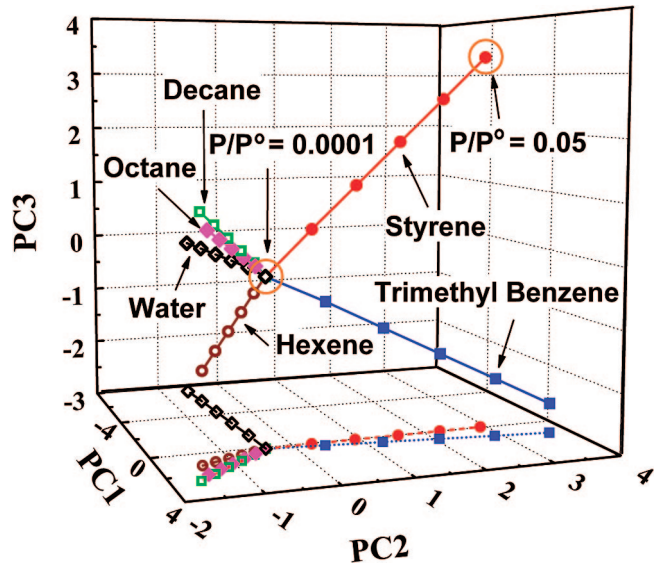

Figure 3. Data in principle component space[24] from a 10-detector array exposed to the representative VOC biomarkers of lung cancer as well as to water (to simulate the humidity effect in the exhaled breath) at $P/P° = 0.0001-0.05$ in air. The first three principal components depicted contained 92% of the total variance in the data. The linear lines contain >90% of the data for each analyte. Each VOC biomarker was presented five times to the array with the order of presentation randomized over all repetitions of all test solvents. For sake of clarity, the projection of the principal component space on PC1 and PC2 is included. The "intersection" point of all curves stands for the response of the array to $P/P° = 0.0001$ analyte concentration. Gradual movement from the "intersection" point to the "periphery" indicates for a gradual increase of the concentration. This way, the closest points to the graph boundaries stand for $P/P° = 0.05$ analyte concentration (for illustration, see the styrene case in the figure).

of the sensors showed increased resistance upon exposure to a certain VOC biomarker, the other part showed decreased resistance upon exposure to the same VOC (see Figure 2). These changes could be attributed basically to one or more of the following mechanisms: (I) charge transfer from

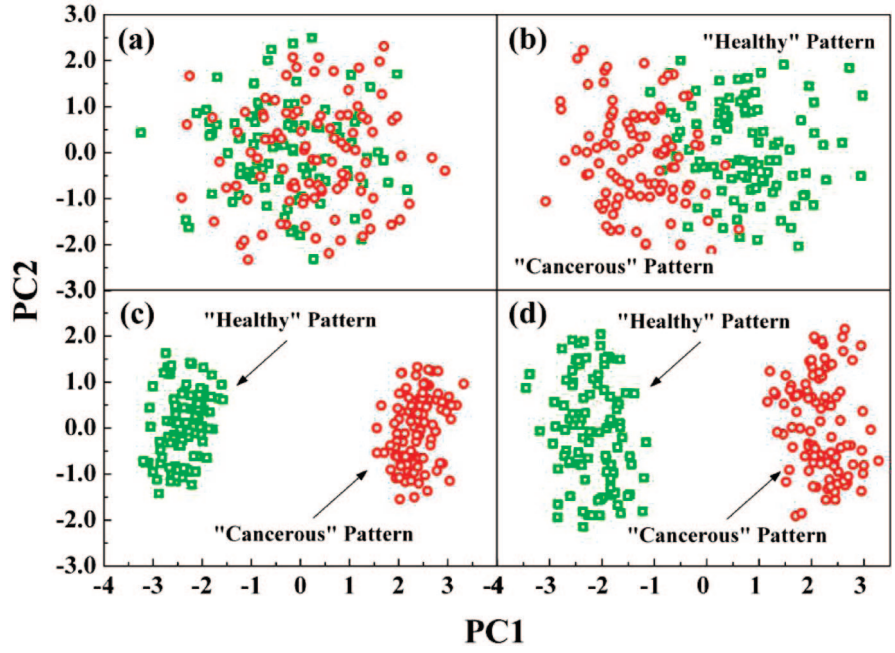

Figure 4. Principal components score plots[27] of an array of 10 sensor films upon exposure to simulated "healthy" and "cancerous" pattern at (a) 80% RH; (b) 10% RH; (c) 1% RH; and at (d) 80% RH and preconcentration of 50 times. The fingerprint data for 80 and 1% RH cases (as two representative samples) are presented in Figure 4a,b of the Supporting Information, respectively.

adsorbed species to the SWCNTs;[14,15] (II) modifications of contact work functions;[16] and (III) carrier scattering by adsorbed species.[17] For the studied array of sensors, we take the view that different interaction between the functional monomers and SWCNTs result in different carrier type and different contact work function.[16,18]

In contrast to the "lock-and-key" approach,[19,20] each of the developed sensors is broadly responsive to a variety of biomarkers and each biomarker produces a distinct fingerprint from the array of broadly cross-reactive sensors (see Figure 2). This allows considerably widening the variety of VOCs to which a given matrix is sensitive, to increase the degree of component identification and to perform an analysis of individual components in complex multicomponent (bio) chemical media.[21] Yet, to acquire information on the identity, properties, and concentration of the vapor exposed to the sensor array, pattern recognition algorithms[22,23] should be applied to the entire set of signals, obtained simultaneously from (all) the sensors (in the array).

Figure 3 presents the concentration-dependent $\Delta R/R_b$ response data for the entire detector array in principle component analysis (PCA)[24] space. Each test VOC biomarker produced a unique signal response pattern with the pattern direction in principle component space diagnostic of the biomarker and the pattern height proportional to the biomarker concentration in the vapor phase. This behavior is further illustrated by normalization of the detector response patterns with respect to analyte concentration according to

$$S_j = \frac{\Delta R_j}{R_{bj}} \cdot \frac{P}{P^0} \qquad (1)$$

where S_j is the normalized signal for 10 sensor films exposed to trimethyl benzene, styrene, decane, octane, and 1-hexene, each presented at $P/P^\circ = 0.0001-0.05$, where P and P° are the partial pressure and vapor pressure of the analyte at room temperature ($\approx$ 21 °C), respectively. The characteristic S_j pattern of each test vapor was maintained, within experimental error, as the analyte concentration was varied (not shown). From these results, one can see that the sensor array response discriminates quite well between the individual VOC biomarkers and water. Furthermore, the results show that the scores for apolar molecules are all on the positive half of the PC1 axis and scores for polar molecules are on the negative half of PC1 axis. Of great interest, the representative nonpolar lung cancer biomarkers (e.g., 1-hexene, octane, and decane) have a negative PC2 score while the other biomarkers show a positive PC2 score. This leads to a clear discrimination of lung cancer biomarkers.

On the basis of the GC-MS analysis of real breath samples (see Figure 1), we prepared simulated "healthy" and "cancerous" breath patterns at similar concentration levels. The simulated breath patterns were prepared in 80 ± 1% RH (where RH = relative humidity) background to simulate the background water vapor content in real human breath. As a simulated "cancerous" breath, we took a mixture of 25.7 ± 1.2 ppb styrene, 32.8 ± 4.7 ppb 1,2,4-trimethyl benzene, 30.0 ± 3.4 ppb decane, 22.1 ± 0.9 ppb octane, and 23.9 ± 3.2 ppb 1-hexene with 80 ± 1% RH, 16 ± 1% O_2, 5 ± 1% CO_2, and 1.0 ± 0.2 ppm CO.[25] As a simulated healthy state, we took 20.1 ± 1.8 ppb decane with 80 ± 1% RH, 16 ± 1% O_2, 5 ± 1% CO_2, and 1.0 ± 0.2 ppm CO. Multiple exposures to each mixture were performed and data were obtained for the array of sensors. PCA of the obtained signal indicated that discrimination between simulated cancerous and healthy breath is rather difficult (Figure 4a; see Figure 4a in the Supporting Information for the fingerprint data). Yet, gradual decrease of the relative humidity content from 80 to 10% formed two adjacent pattern recognition clusters, indicating a start of discrimination between the different

breath samples (Figure 4b). Decreasing the RH from 10 to 1−5% formed well-separated clusters (see Figure 4c; see Figure 4a in the Supporting Information for the fingerprint data) indicating an excellent discrimination capability between simulated "healthy" and "cancerous" patterns. Alternatively, preconcentrating the simulated breath at 80% RH by 50 times[26] resulted in an excellent discrimination capability between the "healthy" and "cancerous" patterns (Figure 4d).[27]

Finally, real breath samples that were preconcentrated by SPME technique or extracted from water were passed through a chamber containing our array of devices for sensor response. On the basis of preliminary results, the PCA analysis of the resistance responses has shown partially overlapping clusters between the various "healthy" breath samples and between the various "cancerous" breath samples, mostly due to different diet, metabolic, and genetic states of the volunteers. No overlapping was observed between the inclusive cluster (i.e., the cluster that delimits the whole responses from all volunteers in a given disease state) of the healthy and cancerous breath samples. Indeed, the PCA data of the "healthy" and "cancerous" states showed two well-separated clusters, similar to those observed in Figure 4c and d, indicating differentiation between the two classes of breath. Experiments with a wider population of volunteers to thoroughly probe and understand the array response to real breath samples considering diet, metabolic, and genetic states are underway and will be published elsewhere.

In summary, our observations indicate that chemiresistive random network of SWCNTs coated with nonpolymeric organic materials has high potential for diagnosis, detection, and screening of lung cancer via breath samples, especially if the sensors array is preceded with either water extractor and/or preconcentrator of VOCs (e.g., SPME). The developed devices are expected to be relatively inexpensive, portable, and amenable to widespread screening, thus help saving millions of lives every year. Given the impact of rising incidence of cancer on health budgets worldwide, the proposed technology will be a significant saving for both private and public health expenditures. The potential for using the proposed technology toward other diseases and conditions will contribute to further significant cost and life savings.

Acknowledgment. The research was funded by the Marie Curie Excellence Grant of the European Commission's FP6, the Israel Cancer Association, and the Technion's Russell Berrie Nanotechnology Institute. The authors acknowledge Professor Abraham Kuten, Dr. Roksolyana Abdah-Bortnyak, and Dr. Salem Billan (Rambam Medical Center, Haifa, Israel) for assistance in breath collection, Dr. Ayelet Fishman (Technion, Israel) for allowing access to her GC-MS, and the reviewers for critical and constructive comments on the ms. H.H. holds the Horev Chair for Leaders in Science and Technology.

Supporting Information Available: Materials, fabrication of sensors, and response measurements of an array of sensors. This material is available free of charge via the Internet at http://pubs.acs.org.

References

(1) Boyle, P.; Ferlay, J. *Ann. Oncol.* **2005**, *16*, 481–488.
(2) Jemal, A.; Murray, T.; Ward, E.; Samuels, A.; Tiwari, R. C.; Ghafoor, A.; Feuer, E. J.; Thun, M. J *CA Cancer J. Clin.* **2005**, *55* (1), 10–30.
(3) Boiselle, P. M.; Ernst, A.; Karp, D. D. *Am. J. Roentgenol.* **2000**, *175* (5), 1215–1221.
(4) Gordon, S. M.; Szidon, J. P.; Krotoszynski, B. K.; Gibbons, R. D.; Oneill, H. J. *Clin. Chem.* **1985**, *31* (8), 1278–1282.
(5) O'Neill, H. J.; Gordon, S. M.; O'Neill, M. H.; Gibbons, R. D.; Szidon, J. P. *Clin. Chem.* **1988**, *34* (8), 1613–1618.
(6) Phillips, M.; Gleeson, K.; Hughes, J. M. B.; Greenberg, J.; Cataneo, R. N.; Baker, L.; McVay, W. P. *Lancet* **1999**, *353*, 1930–1933.
(7) Yu, H.; Xu, L.; Cao, M.; Chen, X.; Wang, P.; Jiao, J.; Wang, Y. *Proc. IEEE Sens.* **2003**, *2*, 1333–1337.
(8) Di Natale, C.; Macagnano, A.; Martinelli, E.; Paolesse, R.; D'Arcangelo, G.; Roscioni, C.; Finazzi-Agro, A.; D'Amico, A. *Biosens. Bioelectron.* **2003**, *18* (10), 1209–1218.
(9) Snow, E. S.; Novak, J. P.; Campbell, P. M.; Park, D. *Appl. Phys. Lett.* **2003**, *82* (13), 2145–2147.
(10) Novak, J. P.; Snow, E. S.; Houser, E. J.; Park, D.; Stepnowski, J. L.; McGill, R. A. *Appl. Phys. Lett.* **2003**, *83* (19), 4026–4028.
(11) Star, A.; Tu, E.; Niemann, J.; Gabriel, J.-C. P.; Joiner, C. S.; Valcke, C. *Proc. Natl. Acad. Sci. U.S.A.* **2006**, *103* (4), 921–926.
(12) Silkoff, P. E.; Deykin, A.; Dweik, R. A.; Laskowski, D.; Baraldi, M. D.; Lundberg, J. O.; George, S. C.; Marczin, N.; Metha, S *Am. J. Respir. Crit. Care Med.* **2005**, *171*, 912–930.
(13) The 10 nonpolymeric organic materials used in this study were selected empirically from a set of 42 compounds, based on two main criterions: (a) providing the highest sensing responses for most of the targeted VOCs, and (b) providing the highest degree of "dissimilarity" between the sensing signals of the various sensors.
(14) Gao, T.; Woodka, M. D.; Brunschwig, B. S.; Lewis, N. S. *Chem. Mater.* **2006**, *18*, 5193–5202.
(15) Li, J.; Lu, Y.; Ye, Q.; Cinke, M.; Han, J.; Meyyappan, M. *Nano Lett.* **2003**, *3* (7), 929–933.
(16) Byon, H. R.; Choi, H. C. *J. Am. Chem. Soc.* **2006**, *128* (7), 2188–2189.
(17) Park, H.; Zhao, J.; Lu, J. P. *Nanotechnology* **2005**, *16* (6), 635–638.
(18) Kuzmych, O.; Allen, B. L.; Star, A. *Nanotechnology* **2007**, *18* (37), 375502/1–375502/7.
(19) Schierbaum, K. D. *Sens. Actuators, B* **1994**, *18* (1−3), 71–76.
(20) Goepel, W. *Mikrochim. Acta* **1997**, *125* (1−4), 179–196.
(21) Martin, M.; Santos, J.; Agapito, J. *Sens. Actuat. B* **2001**, *B 77*, 468–471.
(22) Gardner, J. W.; Bartlett, P. N. *Electronic noses: principles and applications*; Oxford University Press: Oxford, 1999; p 245.
(23) Strike, D. J.; Meijerink, M; G, H.; Koudelka-Hep, M. *Fresenius' J. Anal. Chem.* **1999**, *364*, 499–505.
(24) PCA finds projection weights for sensor response data that maximize total response variance in principal components, where the dimension capturing most sensor variance is given by PC1, and the dimension capturing the second most variance (subject to being orthogonal to PC1) is given by PC2, etc.
(25) Chen, X.; Cao, M.; Li, Y.; Hu, W.; Wang, P.; Ying, K.; Pan, H. *Meas. Sci. Technol.* **2005**, *16*, 1535–1546.
(26) The preconcentration was carried out only for the VOC biomarkers but not for the water. The water content before and after preconcentration remained ∼80% RH.
(27) Water molecules have high chemical and electrical affinity towards SWCNTs. Therefore, at conditions of real breath, the high concentration level of water molecules (80% RH) screens the responses of lung cancer VOCs that exist at lower concentration levels. Bringing either the water molecules (by means of extraction) or the lung cancer VOCs (by means of pre-concentration) to comparable concentration levels allow good discrimination between the different breath states.

NL801577U

Supporting Information for:

Detecting Simulated Patterns of Lung Cancer Biomarkers by Random Network of Single-Walled Carbon Nanotubes Coated with Non-Polymeric Organic Materials

Gang Peng, Elena Trock, and Hossam Haick
The Department of Chemical Engineering and Russell Barrie Nanotechnology Institute, Technion – Israel Institute of Technology, Haifa 32000, Israel.
E-mail: hhossam@technion.ac.il

1. Materials

P-type semiconducting SWCNTs having an average diameter of 1.5 nm and length of 7 μm, with a purity of >90 wt%, were obtained from ARRY international LTD (Germany). Dioctyl phthalate ($C_{24}H_{38}O_4$) plasticizer, propyl gallate ($C_{10}H_{12}O_5$), authracene ($C_{14}H_{10}$), tetracosanoic acid ($C_{24}H_{48}O_2$), tricosane ($C_{23}H_{48}$), 3-methyl-2-phenyl valeric acid ($C_{12}H_{16}O_2$), tris(hydroxymethyl)nitro-methane ($C_4H_9NO_5$), tetracosane ($C_{24}H_{50}$), tetracosanoic acid ($C_{24}H_{48}O_2$), 1.2.5.6.9.10-hexabrormo-cyclododecane ($C_{12}H_{18}Br_6$), and pentadecane ($C_{15}H_{32}$), were all purchased from Sigma-Aldrich and used to functionalize SWCNTs. Decane (>95% purity), octane (>99.0% purity), 1-hexene (>98 %purity), 1,2,4-trimethylbenzene (>98% purity) and styrene (>99.8% purity) were also purchased form Sigma-Aldrich.

2. Fabrication of Sensors

SWCNTs having an average diameter of 1.5 nm and length of 7 μm, were dispersed in DMF, using sonication, and followed by ultracentrifugation. Then, a degenerative p-doped silicon wafer having 2000 nm (in thickness) SiO_2 film was inverted and grazed against a surface of the SWCNTs solution, in a manner that a layer of solution remained on the surface. While still coated with solution, the substrate was blown with stream of dry N_2. This resulted in an optically homogeneous thin film of DMF+SWCNTs. The substrate was then rinsed with deionized H_2O and dried again. This process was repeated several times to yield a desired resistance. After the

deposition of the SWCNT random network, 50 nm Pd electrodes were evaporated through an interdigital shadow mask.

Fig. 1 shows SEM image of the random network of SWCNTs between two adjacent Pd electrodes. From this figure, one can see clearly that the SWCNTs have made up a random network and there are many paths connecting the two adjacent electrodes together by the SWCNTs. Several studies[1, 2] have shown that the intersection of two semiconducting SWCNTs or two metallic SWCNTs forms a good electrical contact with an electrical conductance ~0.1 e^2/h and that the intersection of a metallic and a semiconducting SWCNTs forms a Schottky barrier with a barrier height approximately equal to 1/2 band gap of the semiconducting SWCNT. Consequently, we expect that highly interconnected SWCNT arrays will be electrically continuous with electronic properties that depend on the level of interconnectivity and on the electronic properties of the constituent SWCNTs. The random network geometry has several advantages: it eliminates the problems of nanotube alignment and assembly, eliminates conductivity variations due to nanotube chirality and geometry, and is tolerant to individual SWCNT channel failure because the device's characteristics are averaged over a large number of nanotubes.[1,2]

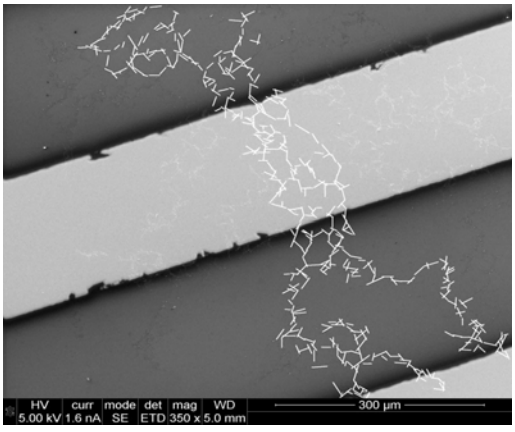

Fig. 1 Magnified segment of SEM image for random network SWCNT contacted by Pd electrodes. For sake of clarity, we highlight in a part of the image the position of SWCNTs by white lines.

After we prepared the electrode with random network of SWCNTs, then a single drop of 10^{-3}M solution of different functional monomers in THF was drop cast on the device. The device was dried for 2h in a fume hood at the ambient temperature, then baked at 50 ºC in an oven.

3. Response Measurements of an Array of Sensors

The developed sensors were mounted into a custom PTFE circuit board which has 10 separated sensor sites and then the board was mounted inside of a stainless steel test chamber with a volume of less than 100 cm^3. An Agilent Multifunction switch 34980 controlled by USB was used to choose the active sensor at a given time. A Stanford Research System SR830 DSP Lock-in amplifier that is controlled by an IEEE 488 system was used to supply the AC voltage signal and measure the corresponding current or resistance - The sensing responses presented in this study were obtained at fixed AV voltage (200 mV, 500 Hz). Using this device setup, we were capable of measuring normalized conductance response values as small as 0.01% [12]. The entire system was controlled by a custom Labview program.

Before staring the sensing experiments, the chamber was brought to a vacuum of 10^{-3}-10^{-4} torr and heated to 37 °C (to resemble the human's body temperature). Then, a computer-controlled automated flow system delivered pulses of simulated biomarker(s) of VOCs at a controlled fraction of the biomarker(s) vapor pressure(s) to the detectors. Oil-free air, obtained from a compressed air source was used as a carrying gas for the VOCs biomarkers. In a typical experiment, signals of sensor array elements was collected for 10 mins of clean air, followed by 10 mins of analyte vapor in air, and then followed by another 10 mins of clean air to purge the system. Data analysis of the signals that were collected from all the sensors in the array were performed using standard principal component and cluster analysis.[3, 4]

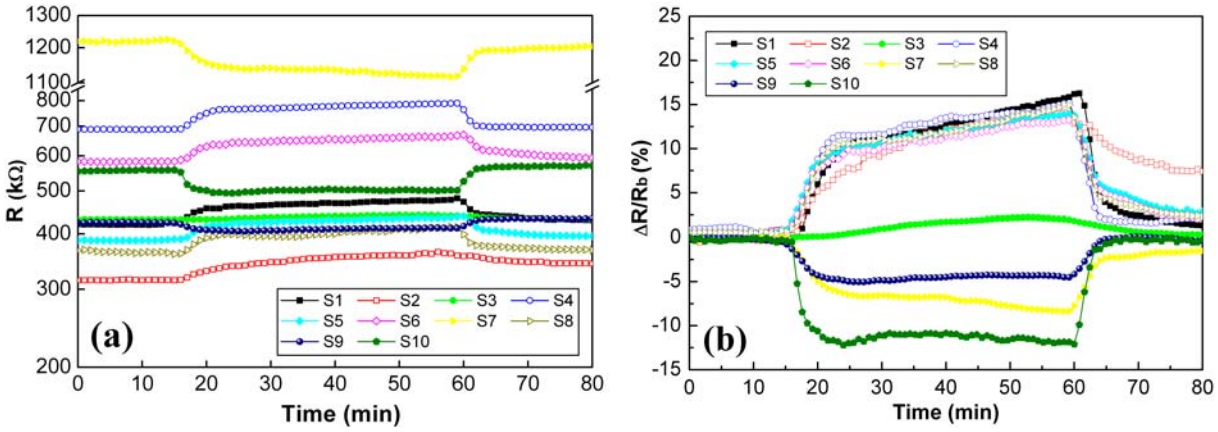

Fig. 2 **(a)** Absolute resistance responses, R, and **(b)** relative differential resistance responses, $\Delta R/R_b$ (where R_b is the baseline resistance of the detector in the absence of analyte, and ΔR is the baseline-corrected steady-state resistance change upon exposure of the detector to analyte), of network of SWCNTs coated with films of different organic monomers, to trimethyl benzene vapor at a concentration of P/P^o = 0.005. The resistance values were obtained at fixed AV voltage (200 mV, 500 Hz).

Fig. 2 shows absolute current response (a) and relative differential resistance responses (b) of a random network of SWCNTs coated with films of organic compounds mentioned in Table 1 above, to trimethyl benzene vapor at concentrations $P/P^o = 0.005$, where P and P° are the partial pressure and vapor pressure of the analyte at room temperature (≈ 21 °C), respectively. As shown in the figure, sorption of biomarkers showed change in resistance and current with exposure to an analyte. Part of the sensors showed increased resistance (decreased current) while other showed decreased resistance (increased current). These changes could be attributed basically to one or more of the following mechanisms: (I) charge transfer from adsorbed species to the SWCNTs;[5,6] (II) modifications of contact work functions;[7] and/or (III) carrier scattering by adsorbed species.[8] For the studied array of sensors we take the view that different interaction between the functional monomers and SWCNTs result in different carrier type and different contact work function.[7,9] The slow response time (on the order of 10s of minutes) can be attributed to the fact that organic films with thicknesses more than 200 nm (as is the case in the studied sensors here, where the films thicknesses range between 0.5 and 1.0 μm) involve significant mass transfer limitations on the VOC molecules within the film – *cf.* refs. 10 and 11.

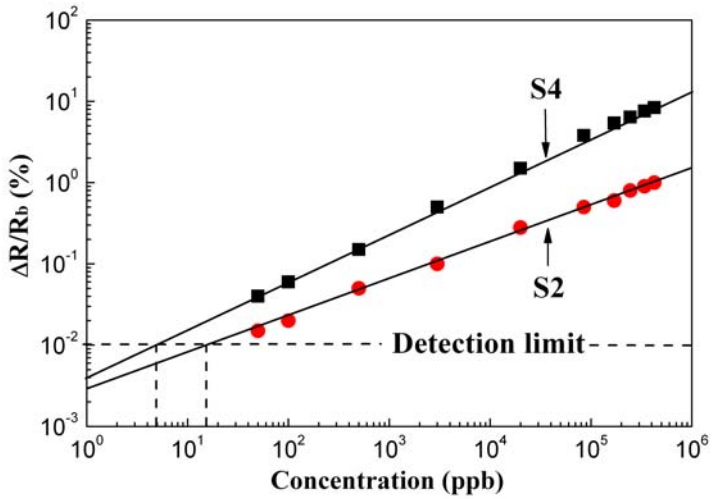

Fig. 3 Response of SWCNT sensors coated with authracene (S2) and tricosane (S4) for decane at various concentration levels. The detection limit of each sensor is shown as the intersection between the dashed line at 0.01% $\Delta R/R_b$ and the linear fit of "$\Delta R/R_b$(%) vs. concentration (ppb)" data (continuous black line).

Fig. 3 shows representative responses of a network of SWCNTs coated with authracene (S2) and tricosane (S4), as representative examples, upon exposure to different concentrations of decane. As could be observed from the figure, the sensors were responsive for a wide range of

concentrations ranging from 10s of ppb to 100s of ppm, and, furthermore, indicated a detection limit of 10-15 ppb, much beyond the concentration level of decane in either "healthy" breath (20.1±1.8 ppb) or "cancerous" breath (30.0±3.4 ppb). In this context, it's noteworthy to point out that the detection limit of a given sensor doesn't depend only on the coating material, but also on the targeted VOC (and, more specifically, on the interaction between the coating material and VOC). For individual sensors that were exposed to a specific VOC (*e.g.*, S5 upon exposure to decane), the detection limit was higher than the concentration of a specific VOC existed in the exhaled breath samples. In this case, the pattern recognition algorithm applied for the array of sensors can discard the "contribution" of such sensors.

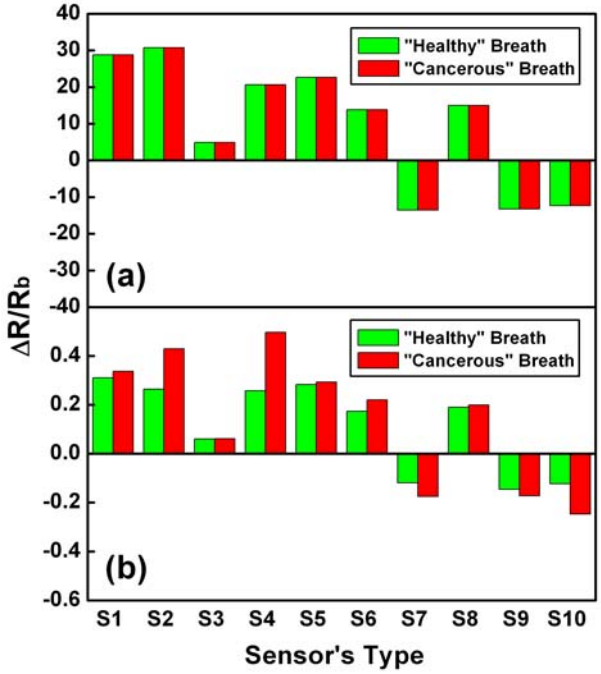

Fig. 4 Response fingerprints of simulated patterns of "healthy" and "cancerous" breath at **(a)** 80% RH and **(b)** 1% RH. The responses of each sensor in the array, for each breath state, are presented.

Fig. 4 shows a response data of simulated pattern of "healthy" and "cancerous" breath at 80% RH (Fig. 4a) and 1% RH (Fig. 4b). At 80% RH, each specific sensor exhibited similar responses upon exposure to "healthy" and "cancerous" VOC patterns (see Fig. 4a). The responses obtained from the different sensors in the array under the same conditions, however, were different. These observations could be attributed to the screening effect of the water molecules. At 80% RH, the water molecules appear in much higher concentrations than the targeted VOCs, and, therefore, the minor differences between the "healthy" and "cancerous"

VOC patterns are undistinguishable. The different interaction and/or absorption of the water molecules with/in the different coating materials, however, cause for different signals from the various sensors. In contrary to these observations, at 1% RH, each specific sensor (excluding S3) exhibited different responses upon exposure to "healthy" and "cancerous" VOC patterns (see Fig. 4b). Furthermore, each sensor exhibited different responses than the other sensor in the same array. This observation could be explained as follows. At 1% RH, the concentrations of water molecules and targeted VOCs are (roughly speaking) comparable, and, therefore, the effect of the latter is (more) perceivable. The significantly lower responses at 1% RH (where $\Delta R/R_b$ ranges between -0.11 to 0.49) than that at 80% RH (where $\Delta R/R_b$ range between -13.6 to 30.7) - at the time the VOCs patterns have not changed - stands in support of these explanations.

REFERNCES:

1. Fuhrer, M. S.; Nygard, J.; Shih, L.; Forero, M.; Yoon, Y.-G.; Mazzoni, M. S. C.; Choi, H. J.; Ihm, J.; Louie, S. G.; Zettl, A.; McEuen, P. L. *Science* **2000,** 288, (5465), 494-497.
2. Snow, E. S.; Novak, J. P.; Campbell, P. M.; Park, D. *Appl. Phys. Lett.* **2003,** 82, (13), 2145-2147.
3. Gardner, J. W. *Sens. Actuat. B* **1991,** B4, (1-2), 109-115.
4. Jurs, P. C.; Bakken, G. A.; McClelland, H. E. *Chem. Rev.* **2000,** 100, (7), 2649-2678.
5. Zhao, J.; Buldum, A.; Han, J.; Lu, J. P. *Nanotechnology* **2002,** 13, (2), 195-200.
6. Li, J.; Lu, Y.; Ye, Q.; Cinke, M.; Han, J.; Meyyappan, M. *Nano Lett.* **2003,** 3, (7), 929-933.
7. Byon, H. R.; Choi, H. C. *J. Am. Chem. Soc.* **2006,** 128, (7), 2188-2189.
8. Park, H.; Zhao, J.; Lu, J. P. *Nanotechnology* **2005,** 16, (6), 635-638.
9. Kuzmych, O.; Allen, B. L.; Star, A. *Nanotechnology* **2007,** 18, (37), 375502/1-375502/7.
10. Gardner, J. W.; Bartlett, P. N., Electronic noses: principles and applications. Oxford University Press: Oxford, 1999; p 245.
11. Stussi, E.; Stella, R.; De Rossi, D. *Sens. Actuat. B* **1997**, 43, (1-3), 180-185.
12. Snow, E.S.; Perkins, F.K. *Nano Lett.* **2005**, 5, (12), 2414-2417.